Surface & Coatings Technology 339 (2018) 14–19

Contents lists available at ScienceDirect

Surface & Coatings Technology

journal homepage: www.elsevier.com/locate/surfcoat

Enhanced repeated frictional sliding properties in 304 stainless steel with a gradient nanostructured surface

Daniel Bernoulli[a], Shan Cecilia Cao[a,b], Jian Lu[b,*], Ming Dao[a,**]

[a] Department of Materials Science and Engineering, Massachusetts Institute of Technology, Cambridge, MA 02139, USA
[b] Department of Mechanical & Biomedical Engineering, City University of Hong Kong, Hong Kong, China

ARTICLE INFO

Keywords:
Surface mechanical attrition treatment (SMAT)
Nanoscale surface deformation
Gradient
Finite element analysis (FEA)
Frictional sliding

ABSTRACT

Surface mechanical attrition treatment (SMAT) is a powerful and practical method to surface-harden metals and alloys through the generation of a gradient nanostructured surface. In this study 304 stainless steel was SMAT processed and the mechanical response upon repeated frictional sliding is studied as well as compared to the mechanical response of untreated as-received 304 stainless steel. The repeated frictional sliding experimental work is complemented by finite-element analysis in order to quantify the stress and strain distribution and to qualitatively determine the elastic-plastic deformation behavior. It is shown that repeated frictional sliding on the SMAT processed 304 stainless steel surface results in smaller residual depth, pile-up height and friction coefficient but higher maximum stresses compared to the as-received 304 stainless steel. After approximately 30 cycles the residual depth increases only minimally with each additional cycle because of strain hardening and increased contact area. At low cycle numbers the frictional sliding track of the as-received 304 stainless steel meanders and forms slip bands adjacent to the sliding track. Due to instability of the gradient structure of 304 SMAT processed stainless steel, asperities are formed in the inner zone of sliding tracks at increasing cycle numbers.

1. Introduction

The ongoing technological progress of devices, machines and structures requires an increasing demand of materials with superior mechanical properties. The surface properties of these materials are particularly important as this outermost zone protects the core material, increases the lifetime and improves the usability. In applications where high or cyclic loads are involved, novel high-performance coatings or surfaces are needed, which require a low wear rate, a high hardness, and a high yield strength. Among other techniques such as shot peening [1], shock loading [2], multiple laser shock processing [3] or ballistic impacting [4], surface mechanical attrition treatment (SMAT) [5] is a powerful method to achieve superior mechanical properties with high hardness and high yield strength. During the SMAT process the surface layer of the sample is subjected to high strain rates. This is achieved by accelerating spherical balls with a vibration generator which results in a large number of impacts on the sample surface over a short period of time. The repeated impacts of these balls create then large plastic strains. A more detailed description of the SMAT process can be found in [6,7]. Depending on the strain-rate which is generated by the SMAT process, dislocation motion, twinning and phase transformation may occur in the material [8,9]. Under sufficiently high impact velocities on 304 stainless steel, it is possible to generate nanotwins and nanograins near the surface and consequently a gradient nanostructured surface [6]. Through these effects the hardness and yield strength can be significantly increased compared to an unprocessed material, while preserving relatively high ductility [6].

The sliding wear behavior of SMAT processed 304 stainless steel shows that the wear behavior depends on the lubrication condition. Under dry sliding the SMAT processed layer is not beneficial in improving the wear resistance whereas under oil immersion SMAT processed surfaces are very effective and enhance the wear resistance by up to 3 times [10]. While the sliding track on the as-received surface hardens during sliding, under the lubricated sliding process plastic deformation plays a more important role because material gets pushed to the edges of the sliding track. Since the SMAT processed surface is harder compared to the as-received surface it provides more resistance to plastic deformation and thus shows better wear resistance [10].

SMAT processed 304 stainless steel surfaces have been reported to have a deleterious influence on the corrosion resistance in 0.6 M NaCl solution. Although the nanocrystalline surface is beneficial in promoting passivation, the increase in surface roughness, stain induced

* Correspondence to: J. Lu, 83 Tat Chee Avenue, Kowloon, Hong Kong, China.
** Correspondence to: M. Dao, 77 Massachusetts Ave, Cambridge, MA 02139, USA.
E-mail addresses: jianlu@cityu.edu.hk (J. Lu), mingdao@mit.edu (M. Dao).

https://doi.org/10.1016/j.surfcoat.2018.01.081
Received 23 October 2017; Received in revised form 26 January 2018; Accepted 28 January 2018
Available online 31 January 2018

martensitic formation and dislocations formation cancel out the beneficial effect of the nanocrystalline surface [11]. However, in a tribocorrosion study with 0.9% NaCl solution, SMAT processed 304 stainless steel surfaces are shown to be effective in reducing material removal compared to as-received surfaces. In addition, during tribocorrosion the treated surfaces have shown to be effective in reducing mechanical and chemical wear [12].

In this study the deformation and failure mechanisms upon repeated frictional sliding on SMAT processed 304 stainless steel is analyzed and compared to as-received 304 stainless steel as well as complemented by computational stress and strain distribution studies. This analysis is on the one hand important from a scientific point as it describes a systematic evolution of the sliding behavior under dry and steady state conditions, and on the other hand 304 stainless steel is used in energy applications, e.g. in nuclear power plants and aerospace engines, where surface treatments are searched to improve usability and to extend the lifetime of structural components.

2. Experimental and modeling setup

For the experimental study AISI 304 stainless steel samples with composition (all in mass %) of 0.04 C, 0.49 Si, 1.65 Mn, 7.8 Ni, 16.8 Cr, 0.37 Mo and 72.85 Fe were used. The microstructure is primarily composed of austenite (fcc) and a small amount of α′-martensite (bcc) [6]. The SMAT process in this study has been performed with 3 mm diameter spherical bearing steel balls, a vibrating frequency of 20 kHz and an exposition time of 60 min. The applied frequency and ball diameter result in an impact velocity of around 10 m/s and an approximate strain rate of $10^{2-}\,10^{3}\,s^{-1}$ near the top treated surface [13]. This plastic strain rate value induced by the SMAT process is known based on a simulation model, which was applied to Type 304 stainless steel [14,15]. With this impact velocity and strain rate a gradient nanostructured surface is generated with nanotwins and nanograins near the surface. Since the strain rate decreases with distance from the surface the grain size increases and the twin density decreases from the surface to the center of the sample where the 304 stainless steel is unaffected by the SMAT process [6,8].

In order to perform nanoindentation and repeated frictional sliding experiments, the as-received and SMAT processed samples were first ground and then polished with 0.04 μm silica suspension which results in a shiny, mirror-like surface. Nanoindentation and repeated frictional sliding was performed with a NanoTest NTX machine (Micro Materials, Wrexham, UK). For the nanoindetation experiments a Berkovich diamond indenter was used and penetration depths from 1 μm to 6 μm were applied. The load-displacement curves were evaluated with the Oliver-Pharr method [16]. For the repeated frictional sliding experiments a conical indenter with an apex angle of 120 degree and a diamond tip radius of 4 μm was used. Repeated frictional sliding was accomplished by multiple scratching in the same sliding track. The indenter was programmed to make 1, 15, 30, and 50 sliding cycles at loads of 250 mN and 450 mN over a track length of 500 μm and at a sliding speed of 5 μm/s. For the first 50 μm the NanoTest NTX ramps up to the load and then slides with the applied load for the remaining 450 μm. From the frictional sliding experiments, the friction coefficient μ was determined as μ = Lateral force/Normal force, which was read out form the NanoTest NTX log file. The residual depth and pile-up height of the frictional sliding tracks were measured with a Dektak profilometer from Bruker. Microstructural analysis was analyzed using a FEI Helios 600 dual beam (FIB/SEM) instrument. In the secondary electron microscopy mode an accelerating voltage of 5 kV and a beam current of 0.34 nA was used.

In order to analyze the stress and strain distribution during a single frictional sliding cycle, finite element analysis (FEA) was conducted with the commercial modeling software Abaqus (version 6.14, Dassault Systèmes, Waltham, MA). The plane strain FEA sliding simulations were performed under displacement controlled conditions, matching the experimental depth when loaded by the 250 mN vertical load on the as-received sample. The same average vertical load was also applied for the SMAT processed 304 stainless steel sample during displacement controlled sliding. To model the gradient structure of the SMAT processed 304 stainless steel a layered structure was built. The input data for the yield strength and the elastic-plastic deformation for each were taken from the nanoindentation and frictional sliding experiments as well as from a previous study on SMAT processed 304 stainless steel [6]. The input parameters for the Young's moduli were 196 GPa for the as-received and 202 GPa for the SMAT processed steel. For both cases a Poisson's ratio of 0.3 was used. When the deformation exceeds the yield strength, plastic deformation occurs with a linear stress-strain dependency and a strain-hardening coefficient of 1.3 GPa per 100% strain which is estimated from the data set reported in [6] and 130 MPa per 100% for the SMAT processed case. In the cited study the same SMAT process and the same SMAT machine was used as in our study. The input parameter for the friction coefficient in the FEA model was taken from the experimental data of the single cycle measurement and is equivalent to 0.56 for the as-received and 0.53 for the SMAT processed steel. We note that the FEA model doesn't intent to be used for explaining the progressively reduced increase in sliding depth. However, the FEA modeling does help with the understanding on how SMAT processing changes the stress and strain distribution under the sliding indenter, during the 1st sliding pass when the largest per-scratch depth increment happens.

3. Results

Nanoindentation measurement revealed a hardness of the as-received 304 stainless steel of 2.47 ± 0.10 GPa (data presented as average value ± standard deviation wherever applicable in this study). This value is within hardness values published for 304 stainless in the literature [6,17,18]. Due to the gradient structure, the hardness of the SMAT processed samples decreases with increasing distance from the treated surface as it is shown in Table 1.

The Young's moduli E was measured from 25 nanoindentation curves to be 195.7 ± 22 GPa for the as-received and 202.1 ± 10 GPa for the SMAT processed 304 stainless steel respectively. Those values are in accordance with the literature for as-received 199.6 GPa [19] and 207.8 GPa for nanocrystalline 304 stainless steel [20] as it is the case on the SMAT processed surface. This small (3%) and statistically insignificant variation (with p-value = 0.18 > 0.05) in measured Young's modulus is expected since SMAT is essentially a strain hardening process and thus the elastic modulus of the different layers can be regarded as uniform and nearly constant [21]. The indentation impression size under the indenter tip is in the order of the grain size of the as-received 304 stainless steel, but much bigger compared to the grain size of the SMAT processed samples. As a result, the measured Young's modulus values on the as-received surface are slightly dependent on the grain orientation and whether the measurement was taken close to the grain boundary. On the SMAT processed surface, however, the measured value is an average over many grains. Thus, the surface appears to be more uniform in the SMAT processed case, which is reflected in a

Table 1
Hardness of SMAT processed 304 stainless steel as function of distance from the surface.

Distance from surface [μm]	Hardness [GPa]
1	6.2 ± 0.1
50	5.8 ± 0.2
100	5.1 ± 0.1
150	4.7 ± 0.1
200	4.3 ± 0.2
300	3.3 ± 0.1
400	2.3 ± 0.2

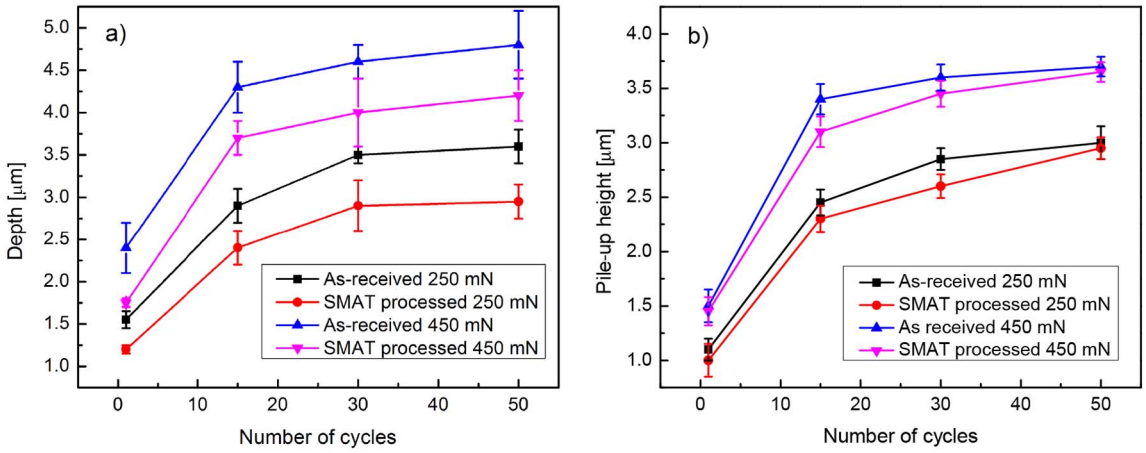

Fig. 1. Residual depth (a)) and pile-up height (b)) as function of number of cycles for SMAT processed and as-received 304 stainless steel measured after repeated frictional sliding at loads of 250 mN and 450 mN respectively.

smaller standard deviation of the reported value.

The residual depth measurements as a function of the number of cycles are presented in Fig. 1a) and show that the residual depth increases with an increased load and cycle number. At cycle numbers > 30, however, the residual depth does not increase significantly for higher cycle numbers. In addition, for the same load and cycle number the SMAT processed 304 stainless steel has a significantly lower residual depth than the as-received 304 stainless steel.

The pile-up height as function of the number of cycles (see Fig. 1b)) shows that the pile-up height increases with load and cycle number. Furthermore, at any given load and cycle number the pile-up height is slightly smaller for the SMAT processed sample compared to the as-received 304 stainless steel. In Fig. 2, the cross sectional material removal as function of the cycle number is presented and indicates that the material removal is bigger for as-received than SMAT processed 304 stainless steel. Similar to the depth and pile-up analysis, the material removal also shows a decreasing incremental change with increasing cycle number.

The friction coefficient analysis (Fig. 3) shows a cycle number as well as a processing condition dependency. The friction coefficient is decreasing with increasing cycle number and is higher for the as-received compared to the SMAT processed 304 stainless steel. At high cycle numbers (> 40), the friction coefficient levels off with values of 0.28 ± 0.03 for the SMAT processed and 0.32 ± 0.03 for the as-received 304 stainless steel.

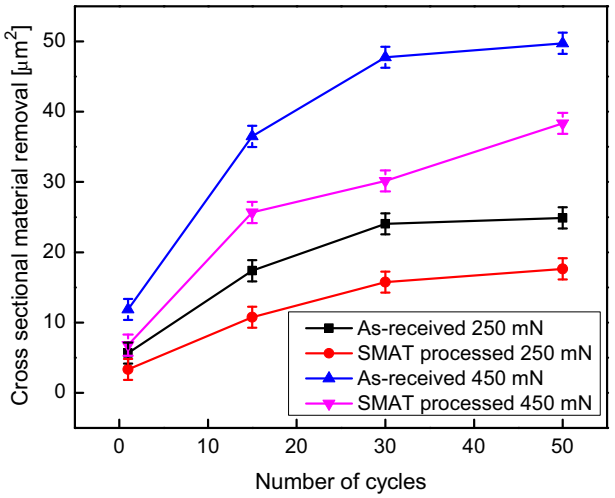

Fig. 2. Cross sectional material removal as function of the number of cycles for as-received and SMAT processed 304 stainless steel.

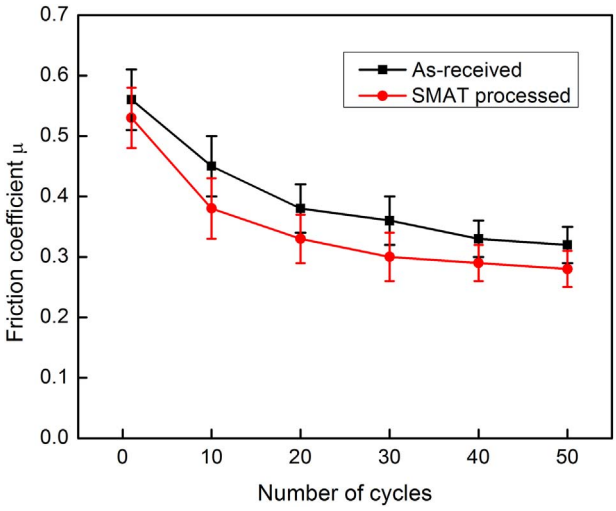

Fig. 3. Friction coefficient as function of the number of cycles for as-received and SMAT processed 304 stainless steel.

Fig. 4 presents the detailed surface morphology of the frictional sliding tracks after 1 cycle at 250 mN of as-received (Fig. 4a)) and SMAT processed (Fig. 4b)) 304 stainless steel and reveals that the tracks are wider on the as-received 304 stainless steel surface compared to the SMAT processed surface. Unlike to the treated surface, the as-received 304 stainless steel (Fig. 4a)) has the tendency to meander and forms slip bands adjacent to the sliding tracks (arrows in Fig. 4a)). With increasing cycle number (Fig. 5a)–c)) more and bigger asperities are formed in the inner zone of the sliding track of the SMAT processed 304 stainless steel.

The maximum stress buildup and distribution during the frictional sliding process was determined by FEA and is presented in Fig. 6 for a single sliding event at equivalent normal force for the as-received and SMAT processed surface. The FEA results show that the maximum von Mises stress is significantly higher for the SMAT processed compared to as-received 304 stainless steel, due to much higher yield strength near the SMAT processed surface. However, the interaction volume where the stress is generated is much bigger for the as-received compared to the SMAT processed 304 stainless steel.

For the same force as in Fig. 6, the equivalent plastic strain is presented in Fig. 7 and confirms that magnitude and interaction volume is increased for the as-received case.

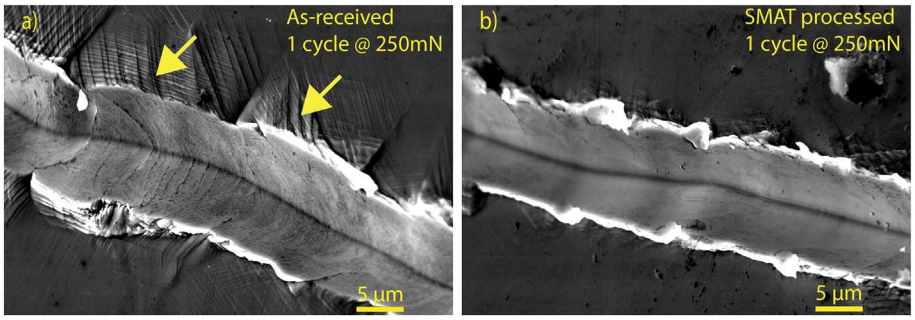

Fig. 4. Secondary electron microscopy images of 1 cycle 250 mN frictional sliding tracks on as-received (a)) and SMAT processed (b)) 304 stainless steel. Compared to the treated steel, the as-received stainless steel meanders and forms slip bands (indicated by arrows) adjacent to the sliding track.

4. Discussion

The SMAT process has two major consequences, which both affect the mechanical response upon repeated frictional sliding: First, SMAT produces nanocrystalline grains and a higher nanotwin density near the surface area and secondly it forms a gradient structure with gradually decreasing hardness and yield strength from the treated nanocrystalline surface to the microcrystalline center of the sample. In addition, the deformation twins induced by the SMAT process play a similar role as grain boundaries in dislocation motion [22,23] and enhance the effect of yield strength increase.

Due to the higher yield strength of nanocrystalline grains compared to their microcrystalline counterparts [24–26], the maximum stress upon repeated frictional sliding at equivalent normal force is higher in the SMAT processed compared to the as-received case as it was confirmed by FEA simulations in Fig. 6. In addition, since the yield strength in the SMAT processed surface is higher, the material is not as prone to undergo plastic deformation, and therefore the volume of stress and strain generation is also smaller compared to the as-received 304 stainless steel. This observation is also confirmed by FEA simulations in Figs. 6 and 7. Furthermore, the increased hardness of the SMAT processed 304 stainless steel results in reduced residual depth upon repeated frictional sliding as it was presented in Fig. 1a).

Upon the frictional sliding process, the interaction volume of the indenter is in the order of the grain size of the as-received 304 stainless steel. Hence, intrinsic effects, such as preferred shearing direction, occur in the microcrystalline grains and form slip band adjacent to the sliding track. This local plastic deformation also increases the variability in the frictional sliding process and creates the meandering at low cycle numbers. Similar phenomena upon repeated frictional sliding were observed in recrystallized Cu and to a larger extend in recrystallized Cu-Zn [27]. Since in the SMAT case the interaction volume of the indenter is much bigger than the size of the nanocrystalline grains no pronounced intrinsic effects occur, and therefore no meandering and slip band formation was observed on the SMAT processed 304 stainless steel surface. However, in both cases at low cycle numbers each repeated frictional sliding event generates plastic deformation, which subsequently results in a strain hardening effect. This is in

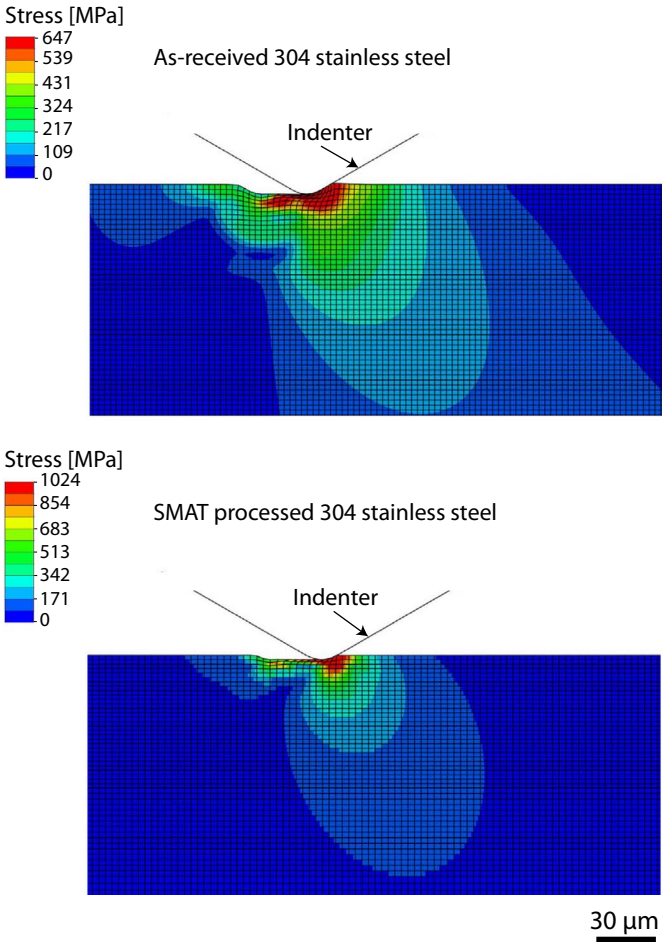

Fig. 6. Stress distribution of as-received (top) and SMAT processed (bottom) 304 stainless steel at equivalent normal force. While the maximum stress is higher in the SMAT processed sample, the stress interaction volume is bigger for the as-received case.

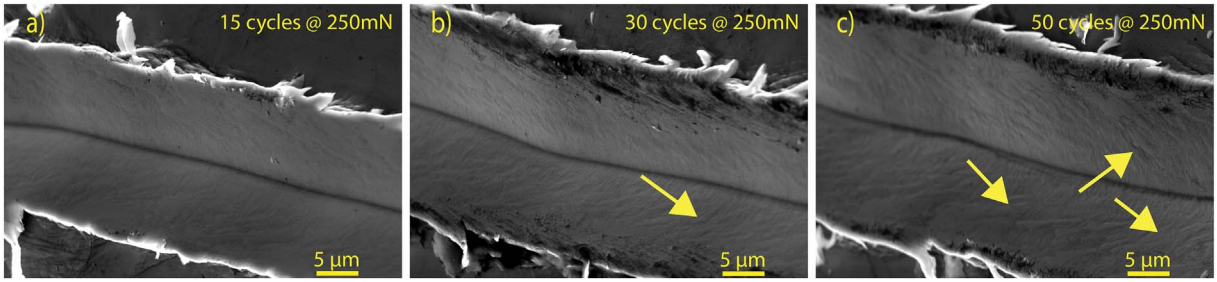

Fig. 5. Secondary electron microscopy images of frictional sliding tracks at 15 (a)), 30 (b)) and 50 (c)) cycles at a load of 250 mN on a SMAT processed 304 stainless steel surface (the 1 cycle sliding track is shown in Fig. 4(b)). With increasing sliding cycles bigger and more asperities are formed in the inner zone of the sliding track. Some asperities are indicated by arrows.

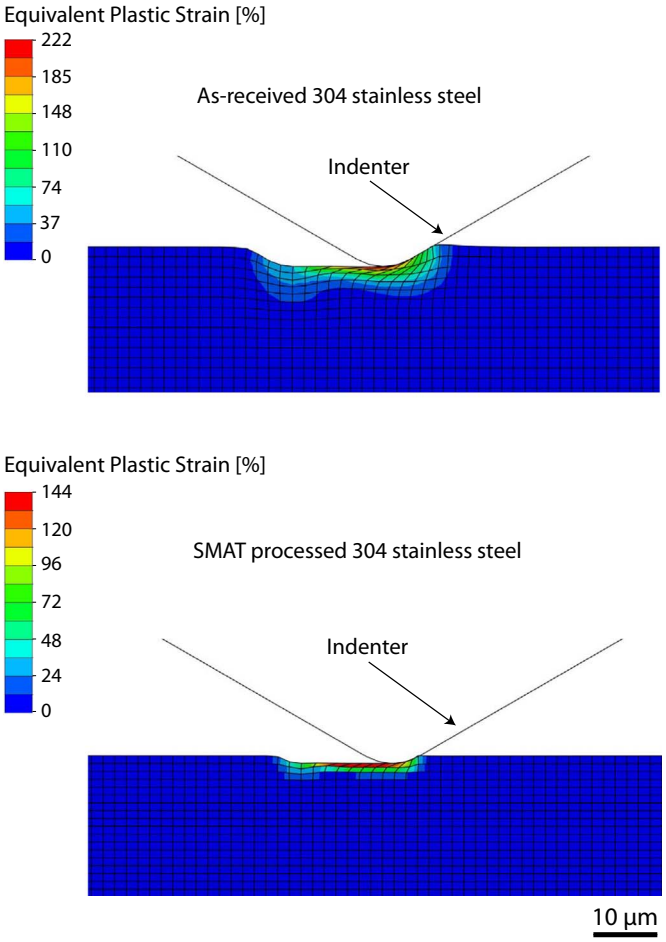

Fig. 7. Equivalent plastic strain for as-received (top) and SMAT processed (bottom) 304 stainless steel upon frictional sliding. The magnitude and interaction volume of the equivalent plastic strain is bigger for the as-received case compared to the SMAT processed 304 stainless steel.

accordance with Ref. [10] where it is shown that the wear track of as-received 304 stainless is markedly hardened during multiple sliding. With increasing cycle number the progressively larger contact area of indenter tip and sample surface becomes an integral part of the process as it is seen in Fig. 1. Because of the increasing contact area and the constant applied load, the maximum stress below the sliding indenter is reduced with each additional cycle. Thus, when all the stresses drop below the yield strength, the change in increased residual depth would be small with each additional sliding. Since a decrease in incremental change of residual depth at cycle numbers > 30 was observed in both as-received and SMAT processed case, it is suggested that the increased contact area is more dominant than the strain-hardening behavior at high cycle numbers. Because the material removal correlates with the residual depth and pile-up height, the curves in Fig. 2 follow the same trend as the curves in Fig. 1.

The increase in surface asperities with increased cycle number in the inner zone of the sliding tracks of SMAT processed 304 stainless steel may be associated with strain localization which results in surface roughening as it was reported in nanocrystalline metals [28,29]. Another possible explanation for the increasing roughness upon repeated frictional sliding of the SMAT processed 304 stainless steel is the gradient structure which can be illustrated by many thin layers stacked on each other with changing yield strengths and shear moduli [28]. As it was shown on repeated frictional sliding on Cu/Au multilayers, a waviness and vortices were observed at higher sliding numbers [30]. The authors in [30] made the analogy to flow patterns under a Helmholtz-Kelvin instability which occurs due to velocity (or in this case shearing) gradient in the layers resulting in mixing. In our case of a gradient structure the grain size increases gradually from the top to the bulk, and so the shear strength changes from the surface to the bulk. We assume that this shear strength gradient results in an instability similar to that found in [30] upon repeated frictional sliding, which creates an intermixing of layers and subsequent asperity creation at higher cycle numbers.

Since nanotwinned Cu [31] exhibits similar values of friction coefficient compared to coarse-grained Cu in spite of different initial microstructure, the decrease in friction coefficient of the SMAT processed compared to the as-received 304 stainless is likely attributed to the nanocrystalline grains near the surface. The relatively small change in friction coefficient from the coarse grained as-received to the nanocrystalline SMAT processed 304 stainless steel is also in agreement with other nanocrystalline metal surfaces as it was shown for Ni [32], Ti [33], and Al [34], even though nanocrystalline metal surfaces have a superior wear resistance compared to their microcrystalline counterparts [24,35]. Furthermore, at our quasi-static sliding speed the friction coefficient of 304 stainless steel is in agreement with previous studies such as Ref. [36].

The pile-up height also scales with the friction coefficient because it is associated with an increase in the interaction forces that pushes the material to the front and sides of the indenter [27]. However, since the difference in friction coefficient of the SMAT processed and as-received 304 stainless steel is small, it is assumed that the effect on the pile-up height is small too. The more important factor on the pile-up height is the refined microstructure [27] as it is the case at the surface of the SMAT processed 304 stainless steel. A nanocrystalline surface reduces the variability in the frictional sliding process and thus the SMAT process has at any given load and cycle number a smaller pile-up height compared to the as-received 304 stainless steel.

5. Conclusion

In this study the mechanical response upon repeated frictional sliding of SMAT processed and as-received 304 stainless is systematically studied. The study shows that the subsequent frictional sliding on a SMAT processed 304 stainless steel surface results in a reduced residual depth, pile-up height, and friction coefficient but higher maximum stresses compared to untreated 304 stainless steel. The reduced friction coefficient can be attributed to the nanocrystalline grains with high hardness near the surface. With this work we anticipate that SMAT processed 304 stainless steel surfaces have the potential to extend the lifetime of components which undergo repeated cyclic loading on the surface as it is the case for e.g. fuel rods in nuclear power plant applications.

Acknowledgments

D.B. acknowledges support from the Advanced Postdoc Mobility Fellowship by the Swiss National Science Foundation, under the grant P300P2_167604. D.B, S.C.C. and M.D. acknowledge support by the Singapore-MIT Alliance for Research and Technology Centre (SMART). S.C.C. and J.L. acknowledge support from NSFC Grant 11572281. J.L. acknowledges financial support provided by the Guangdong Provincial Science and Technology Department under the grant 2014B050504003. The authors thank Dr. Alan Schwartzman from the Nano Lab at MIT for his assistance with the frictional sliding and nanoindentation experiments.

References

[1] J. Lindemann, C. Buque, F. Appel, Effect of shot peening on fatigue performance of a lamellar titanium aluminide alloy, Acta Mater. 54 (4) (2006) 1155–1164.
[2] J.W. Christian, S. Mahajan, Deformation twinning, Prog. Mater. Sci. 39 (1–2) (1995) 1–157.

[3] J.Z. Lu, K.Y. Luo, Y.K. Zhang, G.F. Sun, Y.Y. Gu, J.Z. Zhou, X.D. Ren, X.C. Zhang, L.F. Zhang, K.M. Chen, C.Y. Cui, Y.F. Jiang, A.X. Feng, L. Zhang, Grain refinement mechanism of multiple laser shock processing impacts on ANSI 304 stainless steel, Acta Mater. 58 (16) (2010) 5354–5362.
[4] L. Zhen, G.A. Li, D.L. Zou, W.Z. Shao, Characterization of the deformed microstructure in 1Cr18NiTi stainless steel under ballistic impact, Mater. Sci. Eng. A 489 (1–2) (2008) 213–219.
[5] K. Lu, J. Lu, Nanostructured surface layer on metallic materials induced by surface mechanical attrition treatment, Mater. Sci. Eng. A 375 (2004) 38–45.
[6] A.Y. Chen, H.H. Ruan, J. Wang, H.L. Chan, Q. Wang, Q. Li, J. Lu, The influence of strain rate on the microstructure transition of 304 stainless steel, Acta Mater. 59 (9) (2011) 3697–3709.
[7] J. Lu, K. Lu, Surface nanocrystallization (SNC) of materials and its effect on mechanical behavior, Comprehensive Structural Integrity, 2003.
[8] H.W. Zhang, Z.K. Hei, G. Liu, J. Lu, K. Lu, Formation of nanostructured surface layer on AISI 304 stainless steel by means of surface mechanical attrition treatment, Acta Mater. 51 (7) (2003) 1871–1881.
[9] G.T. Gray, Deformation twinning in Al-4.8 wt-percent mg, Acta Metall. 36 (7) (1988) 1745–1754.
[10] Y. Sun, Sliding wear behaviour of surface mechanical attrition treated AISI 304 stainless steel, Tribol. Int. 57 (2013) 67–75.
[11] T. Balusamy, T. Narayanan, K. Ravichandran, I.S. Park, M.H. Lee, Influence of surface mechanical attrition treatment (SMAT) on the corrosion behaviour of AISI 304 stainless steel, Corros. Sci. 74 (2013) 332–344.
[12] Y. Sun, R. Bailey, Improvement in tribocorrosion behavior of 304 stainless steel by surface mechanical attrition treatment, Surf. Coat. Technol. 253 (2014) 284–291.
[13] K.Y. Zhu, A. Vassel, F. Brisset, K. Lu, J. Lu, Nanostructure formation mechanism of alpha-titanium using SMAT, Acta Mater. 52 (14) (2004) 4101–4110.
[14] H.L. Chan, H.H. Ruan, A.Y. Chen, J. Lu, Optimization of the strain rate to achieve exceptional mechanical properties of 304 stainless steel using high speed ultrasonic surface mechanical attrition treatment, Acta Mater. 58 (15) (2010) 5086–5096.
[15] H.H. Ruan, A.Y. Chen, J. Lu, Characterization of plastically graded nanostructured material: part I. The theories and the inverse algorithm of nanoindentation, Mech. Mater. 42 (5) (2010) 559–569.
[16] W.C. Oliver, G.M. Pharr, Measurement of hardness and elastic modulus by instrumented indentation: advances in understanding and refinements to methodology, J. Mater. Res. 19 (1) (2004) 3–20.
[17] S. Javadi, M. Ghoranneviss, R.S. Rawat, A.S. Elahi, Topographical, structural and hardness changes in surface layer of stainless steel-AISI 304 irradiated by fusion-relevant high energy deuterium ions and neutrons in a low energy plasma focus device, Surf. Coat. Technol. 313 (2017) 73–81.
[18] A. Bahri, E. Kacar, S.S. Akkaya, K. Elleuch, M. Urgen, Wear protection potential of TiN coatings for 304 stainless steels used in rotating parts during olive oil extraction, Surf. Coat. Technol. 304 (2016) 560–566.
[19] C. Caer, R. Pesci, Local behavior of an AISI 304 stainless steel submitted to in situ biaxial loading in SEM, Mater. Sci. Eng. A 690 (2017) 44–51.
[20] J. Frontan, Y.M. Zhang, M. Dao, J. Lu, F. Galvez, A. Jerusalem, Ballistic performance of nanocrystalline and nanotwinned ultrafine crystal steel, Acta Mater. 60 (3) (2012) 1353–1367.
[21] H.H. Ruan, A.Y. Chen, H.L. Chan, J. Lu, Characterization of plastically graded nanostructured material: part II. The experimental validation in surface nanostructured material, Mech. Mater. 42 (7) (2010) 698–708.
[22] L. Lu, X. Chen, X. Huang, K. Lu, Revealing the maximum strength in nanotwinned copper, Science 323 (5914) (2009) 607–610.
[23] K. Lu, L. Lu, S. Suresh, Strengthening materials by engineering coherent internal boundaries at the nanoscale, Science 324 (5925) (2009) 349–352.
[24] K.S. Kumar, H. Van Swygenhoven, S. Suresh, Mechanical behavior of nanocrystalline metals and alloys, Acta Mater. 51 (19) (2003) 5743–5774.
[25] E. Arzt, Overview no. 130 - size effects in materials due to microstructural and dimensional constraints: a comparative review, Acta Mater. 46 (16) (1998) 5611–5626.
[26] J.R. Greer, Nanotwinned metals it's all about imperfections, Nat. Mater. 12 (8) (2013) 689–690.
[27] S.C. Bellemare, M. Dao, S. Suresh, Effects of mechanical properties and surface friction on elasto-plastic sliding contact, Mech. Mater. 40 (4–5) (2008) 206–219.
[28] M.A. Meyers, A. Mishra, D.J. Benson, Mechanical properties of nanocrystalline materials, Prog. Mater. Sci. 51 (4) (2006) 427–556.
[29] X. Chen, Z. Han, X.Y. Li, K. Lu, Lowering coefficient of friction in Cu alloys with stable gradient nanostructures, Sci. Adv. 2 (12) (2016).
[30] Z.P. Luo, G.P. Zhang, R. Schwaiger, Microstructural vortex formation during cyclic sliding of Cu/Au multilayers, Scr. Mater. 107 (2015) 67–70.
[31] A. Singh, N.R. Tao, M. Dao, S. Suresh, Repeated frictional sliding properties of copper containing nanoscale twins, Scr. Mater. 66 (11) (2012) 849–853.
[32] S.V. Prasad, C.C. Battaile, P.G. Kotula, Friction transitions in nanocrystalline nickel, Scr. Mater. 64 (8) (2011) 729–732.
[33] M. Wen, C. Wen, P.D. Hodgson, Y.C. Li, Tribological behaviour of pure Ti with a nanocrystalline surface layer under different loads, Tribol. Lett. 45 (1) (2012) 59–66.
[34] Z.N. Farhat, Y. Ding, D.O. Northwood, A.T. Alpas, Effect of grain size on friction and wear of nanocrystalline aluminum, Mater. Sci. Eng. A 206 (2) (1996) 302–313.
[35] Y.S. Zhang, Z. Han, K. Wang, K. Lu, Friction and wear behaviors of nanocrystalline surface layer of pure copper, Wear 260 (9–10) (2006) 942–948.
[36] S. Kataria, N. Kumar, S. Dash, A.K. Tyagi, Deformation of SS 304 LN during scratch test and influence on evolution of coefficient of friction, Adv. Tribol. 2009 (2009) 648075.